Impact Load Response of PC Rail Joint Sleeper under a Passing Train

Goto, Keiichi; Minoura, Shintaro; Watanabe, Tsutomu; Ngamkhanong, Chayut; Kaewunruen, Sakdirat

DOI:
10.1088/1742-6596/1106/1/012008

Impact Load Response of PC Rail Joint Sleeper under a Passing Train

K Goto[1,2], S Minoura[2], T Watanabe[2], C Ngamkhanong[1] and S Kaewunruen[1]

[1] The University of Birmingham, Edgbaston, UK
[2] Railway Technical Research Institute, Tokyo, Japan

E-mail: goto.keiichi.90@rtri.or.jp

Abstract. The purpose of this study was to clarify the influence of an impact load caused by a train passing over a rail joint on a prestressed concrete (PC) sleeper. In this study, we conducted a three-dimensional finite element (FE) model of the PC sleeper, which was able to simulate its nonlinear behaviour. Using this numerical analytical model, the influence of the impact load caused by the rail joint on the maximum bending moment and stress generated in the sleeper for various irregularities and train speeds were quantitatively evaluated. This study clarified the following items: 1) No cracks occurred in the PC sleeper under the rail surface irregularity actually measured in the field; 2) The crack generated owing to a train running at a speed of 87 km/h when the rail surface irregularity was three times the measured value (the maximum dimension of the irregularity was 7.05mm); 3) The bending moment of the PC sleeper had the characteristic of speed dependency, which was regarded as an influence of the rail surface irregularity.

1. Introduction

The design of prestressed concrete (PC) sleepers is carried out in consideration of the influence of impact loads. Impact loads are caused by rail joints, welded rail joints, track irregularities on the rail surface and wheel flats (damage generated on the wheel treads when the wheels slide on the rail running surface). Among them, impact loads caused by rail joints and wheel flats tend to be relatively large. In Japan, since the beginning of the development of the PC sleeper, wheel flats have been recognized as one of the leading causes of impact loads. Studies on the influence of the impact load caused by the wheel flats on PC sleepers have also been actively conducted [1]. On the other hand, there have been few studies on the influence of the impact load caused by a rail joint on a PC sleeper.

In a previous study, a numerical analysis with a beam model was conducted, and the effect of the impact load caused by a rail joint on a PC sleeper was evaluated [2]. This previous study indicated that the supporting condition of the PC sleeper has a significant influence on the generated bending moment in the sleeper.

However, studies on the cracks generated in a PC sleeper due to the impact load and the influence of wear on the bottom surface of the sleeper, the pre-stressing force, corrosion of the PC steel wire and deterioration of the concrete are inadequate. To evaluate these influences using numerical analysis, it is necessary to construct a three-dimensional finite element (FE) model, taking account of the nonlinearity of the sleeper material.

Based on the above background, we focused on the rail joint and constructed a nonlinear three-dimensional FE model to evaluate the dynamic and nonlinear behaviours of a PC sleeper for a rail

joint. Using this model as a fundamental study, the influences of an irregularity on the rail surface and train speed on the bending moment and stress in a sleeper for a rail joint were quantitatively evaluated.

2. Methodology

2.1. Target PC sleeper

Figure 1 shows the outline of the target track structure. In this section, standard rails of 25m in length and 60 kg/m in weight were used and there was a rail joint at every 25m. PC sleepers in the plane section were Type-6 PC sleepers and those at each rail joint were specifically designed for rail joints. Both of these types are specified in the Japanese Industrial Standards (JIS). The number of PC sleepers per 25-m rail was 41.

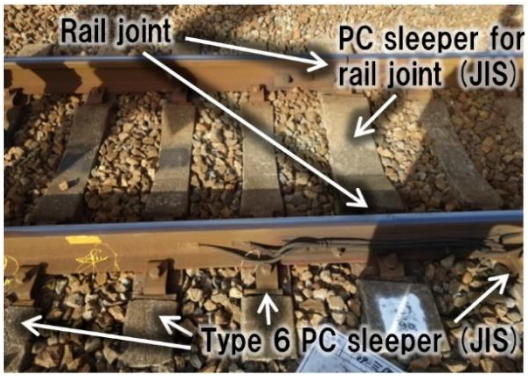

Figure 1. Target track structure.

Figure 2 shows the attachment positions of strain gages for field measurement to obtain the bending moment of the PC sleeper under a passing train, and Fig. 3 shows the attachment positions of the acceleration meters to evaluate the vibration mode of the sleeper. In order to compare the measurement results of the actual sleeper with the results of the numerical analysis, the bending moment and vibration mode of the sleepers during a passing train were measured. For the measurement of the bending moment, the strain gauges were attached to the cross-section at the rail position and the cross- section at the middle of the sleeper. The bending moment at each cross-section was calculated from the measured strains. For the measurement of the vibration mode, five piezoelectric accelerometers (PV-85, Rion) were placed at the positions shown in Fig. 3, and the free vibration response was measured using an impulse hammer. The identification method of the vibration mode was the eigensystem realization algorithm (ERA) method [3]. Trains running on this line were commuter trains for the 1067-mm gauge line, and the wheel load is approximately 50 kN.

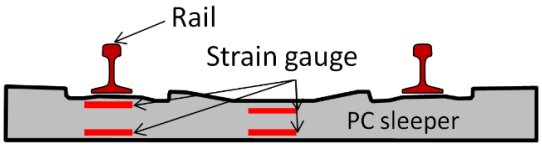

Figure 2. Attachment positions of the strain gauges.

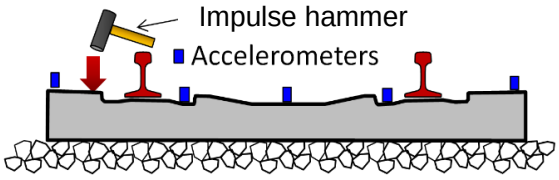

Figure 3. Attachment positions of the acceleration meters.

2.2. Analysis model

Figure 4 shows the outline of the numerical analysis model, and Fig. 5 shows the analysis model of the PC sleepers around the rail joint. In this numerical analysis, a three-dimensional nonlinear FEM analysis was performed using the LS-DYNA (ver. R 8.0.0). For each vehicle, the car, two bogies and

four wheel axles were modelled as rigid body. These rigid bodies were connected with springs and dampers. The rail was modelled with beam elements. Around the rail joint, the rails were divided into 30 elements between rail fastening devices. For other sections, the rails were divided into 30 elements between rail fastening systems. The concrete of the PC rail joint sleeper was modelled with hexahedral solid elements. The PC steel wires and stirrups were modelled with beam elements. The connection between the concrete elements, PC steel wire elements and stirrup elements was assumed to be a perfect bond condition. The Type-6 PC sleeper was modelled as beam elements. The pre-stressing force of the PC rail joint sleeper was reproduced by giving an initial tensile stress to each PC steel wire. The number of elements was 10792, and the number of nodes was 13271.

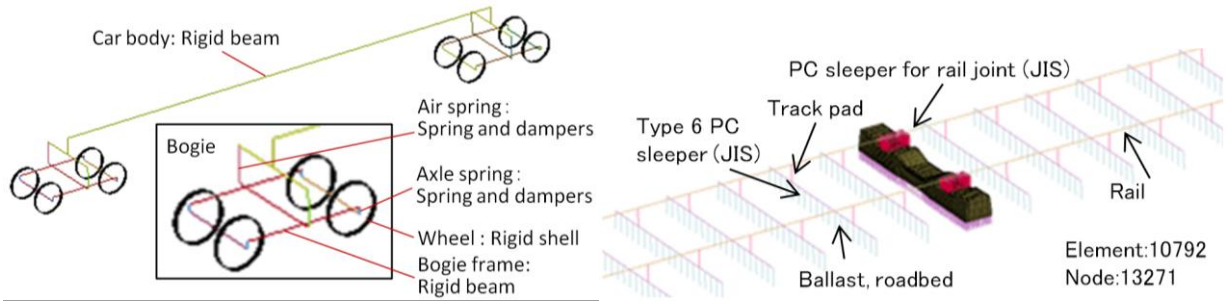

(a) Analysis model of train (b) Analysis model of track structures

Figure 4. Outline of numerical analysis model.

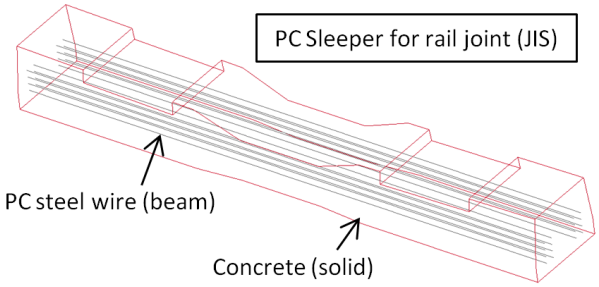

Figure 5. Analysis model of PC sleeper for rail joint.

Figure 6 shows the surface irregularities at the rail joint section. In order to study the influence of the impact force generated by them, the irregularities on the rail surface around the joint were measured using a device with a measurement length of 1.0 m. The measured irregularities were input to the analysis model.

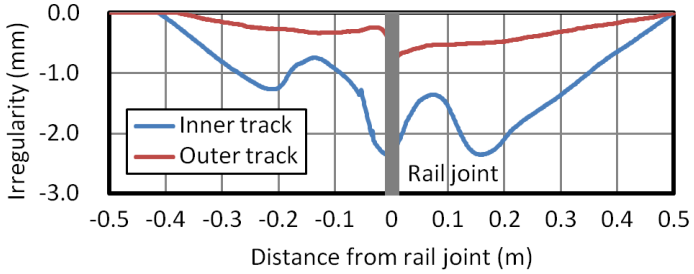

Figure 6. Rail surface irregularities at the rail joint section.

Table 1 shows the material properties used in the numerical analysis. The properties of the respective materials were based on the design standards for Japanese railway structures and track structures [4] [5]. Based on the vibration modes of the PC sleeper and the measurement results of the generated bending moment, the spring constant of the track pad was set to twice the nominal value and the spring constant of the support of the sleeper was set to a value corresponding to the centre-supported state.

Table 1. Material properties used in the analysis.

Rail	Type: 60-kg rail (JIS) Young's modulus E_S: 200 MPa
Track pad	Spring constant D_P: 220 MN/m
Type 6 PC sleeper (JIS)	PC steel wire: 2.9-mm dai. *3-stranded wire, 12 Length L_P: 2000 mm, bottom width B_P: 240 mm Height H_P: 170 mm (rail), 150 mm (middle) Young's modulus (concrete) E_C: 49.5 GPa
PC rail joint sleeper (JIS)	PC steel wire: 2.9-mm dia. *3-stranded wire, 16 Length L_P: 2000 mm, bottom width B_P: 300 mm Height H_P: 170 mm (rail), 145 mm (middle) Young's modulus (concrete) E_C: 49.5 GPa Tensile strength of concrete: 3.08 MPa
Ballast	Ballast thickness h: 250 mm Spring constant D_B: 180 MN/m (for 1 rail)
Roadbed	Ground reaction force coefficient K_{30}: 110 MN/m^3 Spring constant D_S: 111 MN/m (for 1 rail)

2.3. Analysis case

Table 2 shows the details of the analysis case. In this study, the influences of the rail surface irregularity and train speed were evaluated. The rail surface irregularity was based on the measured values (the maximum dimension of the irregularity was 0.72 mm for the outer rail and 2.35 mm for the inner rail). In addition, the analysis was executed for cases which the rail surface irregularity doubled and was three times as large as the measured value. The train running speed in the base case was set to 87 km/h, which was the speed at the time of measurement.

Table 2. Analysis case.

Train speed V	30–130 km/h (87 km/h for basic case)
Rail surface irregularity δ	• Measured value (maximum 0.72 mm for outer rail, maximum 2.35 mm for inner rail), • Twice the measured value • Three times the measured value • Four times the measured value

3. Analysis result and discussion

3.1. Vibration modes of the PC sleeper

Table 3 shows a comparison of the natural frequencies of the PC sleeper for a rail joint. Figure 7 shows the vibration mode forms of such a sleeper. Comparing the natural frequencies of the

measurement results with the numerical analysis results, excluding the rotation mode, the difference between them was within about five percent.

Table 3. Comparison between the measurement and analysis of vibration modes of the PC rail joint sleeper.

Vibration mode	Vertical translation	Rotation	1st mode	2nd mode	3rd mode
Measured (Hz)	101	74	202	534	907
Analysis (Hz)	99	89	199	513	925

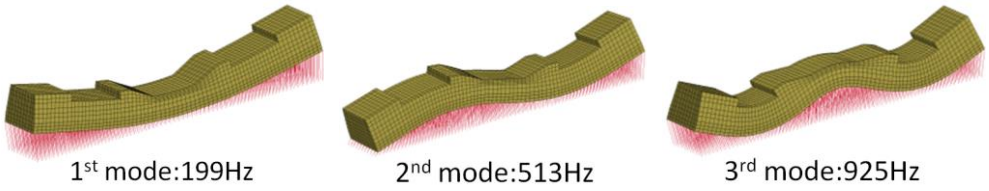

Figure 7. Vibration mode form of the PC sleeper for the rail joint.

3.2. Bending moment on the PC sleeper

Figure 8 shows a comparison between the measurement results and numerical analysis results by means of the time history waveform of the bending moment on the PC rail joint sleeper when a train was passing. As shown in the figure, the maximum value of the negative bending moment occurred at the middle of the PC sleeper is larger than that of the positive bending moment at the rail position of the outer rail. It was also confirmed that although a negative moment instantaneously occurred at the rail position in the numerical analysis, the numerical analysis results and measurement results generally agreed with each other.

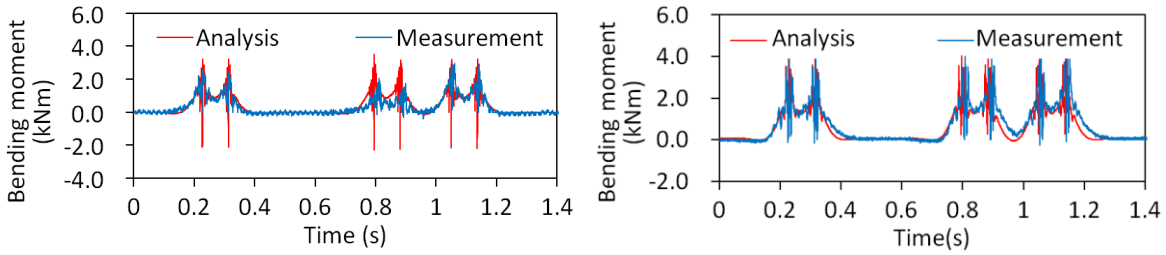

(a) Positive bending at rail position (outer rail) (b) Negative bending at the middle of the sleeper

Figure 8. Comparison between the measurement and the numerical analysis.

3.3. Stress in the concrete and the PC wire

Figure 9 shows the time history of the concrete element stresses in the longitudinal direction of the PC rail joint sleeper. From the figure, it was confirmed that each concrete element has an initial compressive stress owing to the pre-stressing force and that no tensile stress generates on any concrete element even when a train passes.

Figure 10 shows the time history of the axle stress of the PC steel wire. The axle stress is the stress of the element in which the maximum value was observed. It was confirmed that the initial stress generated owing to added initial tensile stress and that the maximum stress was less than the yield stress (1619 MPa), the stress amplitude was approximately 20 MPa.

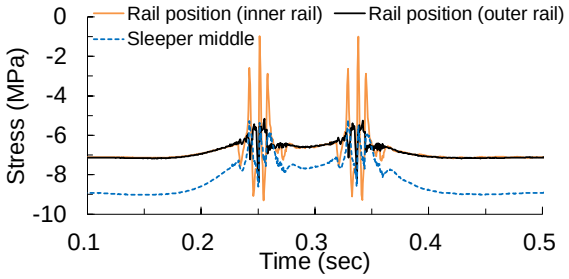

Figure 9. Time history of the concrete element stresses in the longitudinal direction of the PC sleeper.

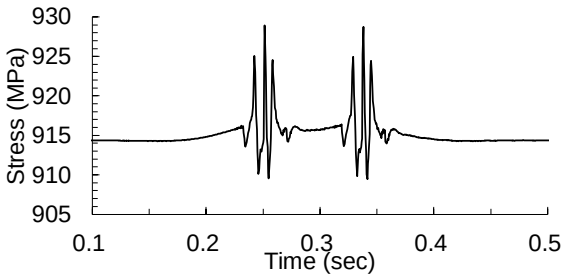

Figure 10. Time history of the axle stress in the PC steel wire.

3.4. Influence of rail surface irregularities and train speed

Figure 11 shows the influence of rail surface irregularities on the maximum bending moment. The figure also shows the decompression moment and crack generation moment used in the design for positive bending at the rail position and negative bending at the middle of the sleeper. From the figure, it was confirmed that the maximum bending moment increased as the irregularity became larger in all the cases. Moreover, the generated moment at the rail position of the inner rail side exceeded the crack generation moment to be considered in the design when the rail surface irregularity is three or more the measured value. For the bending moment at the rail position cross section on the inner rail side, the generated moment in the case when the rail surface irregularity is four times the measured value is smaller than that in the case when the irregularity is three times the measured value. This is thought to be the influence of the train speed, as described below.

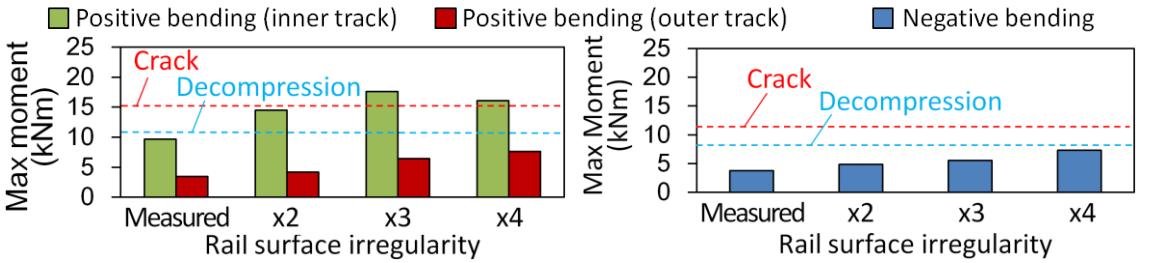

(a) Positive bending at rail position (b) Negative bending at the middle of the sleeper

Figure 11. Influence of rail surface irregularities on the maximum bending moment

Figure 12 shows the influence of the train running speed on the maximum bending moment for various amounts of the rail surface irregularity. From the figure, the maximum bending moment tends to increase with the increase of the rail surface irregularity and train speed. However, for the maximum bending moment at rail position, there is a peak observed at a running speed of around 70 km/h in the base case and there are peaks observed at running speeds of around 30 km/h, 70 km/h and 120 km/h in the case where the rail surface irregularity is four times the measured value. This confirms that there was speed dependence with respect to the bending moment. Although the profile of the measured irregularity on the surface of the inner rail was not a simple shape, it could be seen that rail surface dropped 2.35 mm of the end of the length of the rail of about 0.4 m. Therefore, during the time in which the wheel took to fall freely by 2.35 mm and the time in which the train took to move 0.4 m along the rail coincided with each other, the amount of wheel drop became maximum and the generated maximum moment was expected to increase. The train speed corresponding to this case was about 65km/h for the measured rail surface irregularity, about 46 km/h for the case in which the rail surface irregularity was twice the measured value and about 33 km/h for the case in which the rail

surface irregularity was four times the measured value. In each analysis case, since a peak appeared at these speeds, the maximum generated moment was considered to be influenced by the shape of the rail surface irregularity.

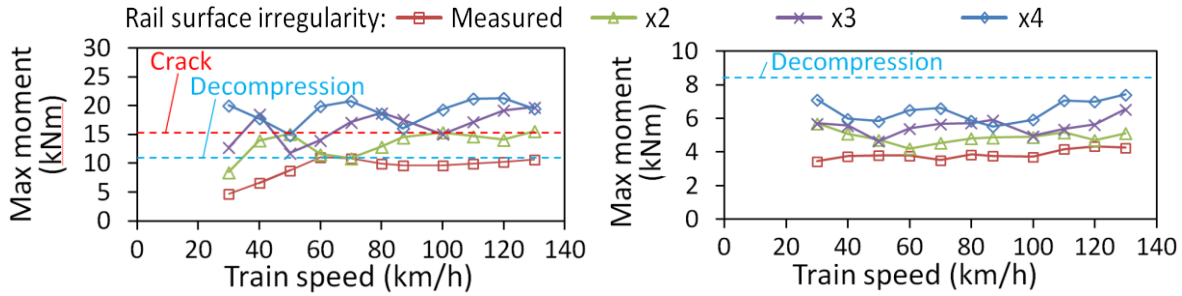

(a) Positive bending at rail position (b) Negative bending at the middle of sleeper

Figure 12. Influence of train running speed on the maximum bending moment for various amounts of rail surface irregularity.

4. Conclusions

In this study, we conducted a nonlinear three-dimensional FE model reproducing the PC rail joint sleeper. Using this model, the influences of the rail surface irregularities and train speed on the bending moment and the stress of the PC rail joint sleeper were quantitatively evaluated.

- According to the numerical analysis using the measured irregularity of the rail surface, no crack generated owing to the train running at a speed of 87 km/h when the rail surface irregularity was as large as the measured value.
- According to the numerical analysis using the measured rail surface irregularity, the crack generated owing to the train running at a speed of 87 km/h when the rail surface irregularity was three times the measured value (the maximum amount of the irregularity on the inner rail side was 7.05 mm).
- The bending moment of the PC sleeper had the characteristics of speed dependency, which is regarded as an influence of the rail surface irregularity.

We will take these findings into the consideration in the design of the PC sleeper and build an optimal design method for PC rail joint sleeper to cope with the impact load caused by rail joints in the future research.

References

[1] Wakui H and Okuda A 1999 A study on limit state design method for prestressed concrete sleepers *Concrete library of JSCE* **33** 1-25

[2] Watanabe T, Matsuoka K and Minoura S 2016 Numerical analysis for the dynamic response characteristics of the prestressed concrete sleeper *VII European Congress on Computational Methods in Applied Sciences and Engineering (ECCOMAS Congress)*

[3] Matsuoka K, Kaito K and Ishii H 2012 Statical consideration regarding the vibration characteristics and vibration factors of 24-span steel railway bridge in 86 years in service *Journal of Japan Society of Civil Engineers F4* 68 3 157-74

[4] Railway Technical Research Institute 2004 *Design Standards for Railway Structures and Commentary (Concrete Structures)* (Tokyo: Maruzen)

[5] Railway Technical Research Institute 2012 *Design Standards for Railway Structures and Commentary (Track Structures)* (Tokyo: Maruzen)